Tunable Signal Processing through a Kinase Control Cycle: the IKK Signaling Node

Marcelo Behar[†‡] and Alexander Hoffmann[†‡]*

[†]Signaling Systems Laboratory, Department of Chemistry and Biochemistry, and [‡]San Diego Center for Systems Biology, University of California at San Diego, La Jolla, California

Submitted September 6, 2012, and accepted for publication May 2, 2013.

*Correspondence: ahoffmann@ucsd.edu

Supporting Material

Contents

Supplemental Figures

Pharmacological inhibition of the IKK cycle components

SC-514 is an IKK2 inhibitor that binds at the conserved ATP-binding pocket and was previously reported to display good selectivity *in vitro*, but has limited bioavailability and an extremely short half-life (1). In our hands SC-514 has little effect in inhibiting overall IKK activity in fibroblasts (Fig. S1 A). However, preliminary experiments show that upon treatment late, but no early, IKK activity is elevated in response to cytokine Tumor Necrosis Factor (TNF) presumably because SC-514 inhibits the IKK2 self-inhibitory C-terminal phosphorylation mechanism (2,3).

We have also observed that pre-treatment of murine fibroblasts with TNF and the phosphatase PP2A inhibitor Calyculin A results in reduced IKK activity (Fig. S1 B). Co-treatment does not seem to have an effect. This result is consistent with previously reported observations using other inhibitors and cell lines (4) and supports the interpretation that dephosphorylation is a necessary step for continuous IKK activation (2) as pre-treatment, in the presence of any basal activity, would trap IKK in the inactive state.

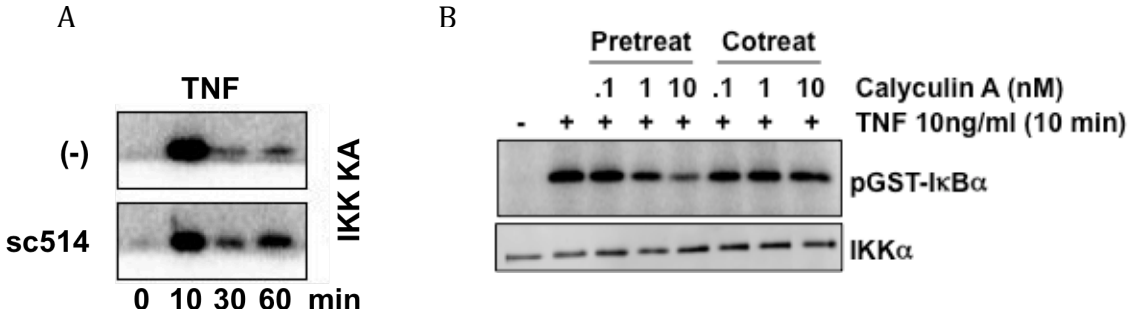

Figure S1. Effect of pharmacological inhibitors on IKK activity. (A) wt Murine Embyonic Fibroblasts were pre-treated with 100μM SC-514 for 30 min prior to stimulation with TNF (1ng/ml). IKK activity was monitored via IP-Kinase Assay (5). SC-514 treatment resulted in only a subtle decrease of TNF-induced IKK activity at 10 min but late activity was dramatically increased. (B) wt MEFs were pre-treated with varying doses of the PP2A inhibitor Calyculin A for 30 min, or co-treated along with a 10ng/ml dose of TNF for 10 minutes. IKK activity was measured using an IP-Kinase Assay. In pre-treated cells, IKK activity was diminished upon increasing Calyculin A concentrations, whereas the co-treatment had no effect.

Analytical solution of the linear three-state cycle

The linear three-state cycle is defined by equations 1-3 (main text). The constant k_2 in these equations can be incorporated into a modified time variable defined as

$$\hat{t} = k_2 t \tag{S1}$$

This transformation is equivalent to setting the units of time to k_2. The factor k_2 that results from expressing the time derivative on the LHS of the differential equations in terms of the modified time can be combined with the other kinetic constants to yield the following modified system:

$$\frac{d[IKK]}{d\hat{t}} = -\frac{k_1}{k_2} s \times [IKK] + \frac{k_3}{k_2}[IKKi] \tag{S2}$$

$$\frac{d[IKKa]}{d\hat{t}} = \frac{k_1}{k_2} s \times [IKK] - \frac{k_2}{k_2}[IKKa] \tag{S3}$$

$$\frac{d[IKKi]}{d\hat{t}} = \frac{k_2}{k_2}[IKKa] - \frac{k_3}{k_2}[IKKi] \tag{S4}$$

Explicit dependence on k_2 can then be eliminated by writing the equations in terms of the ratios k_1'=s k_1/k_2 and $k_3'=k_3/k_2$. The system can be studied in terms of those transformed constants without loss of generality. In the linear case the concentrations can be transformed into fractions of the total pool of IKK dividing the LHS and RHS by IKK_{TOTAL}, assumed here to be conserved, to yield:

$$\frac{dIKK}{d\hat{t}} = -k_1' \times IKK + k_3'(1 - IKK - IKKa) = -(k_3'+k_1')IKK - k_3' IKKa + k_3' \tag{S5}$$

$$\frac{dIKKa}{d\hat{t}} = k_1' \times IKK - IKKa \tag{S6}$$

, where specie's names without square brackets represent the fraction of total IKK. For a square step stimulus and zero initial condition, this of linear equations can be solved using standard methods to yield for IKKa:

$$IKKa(\hat{t}) = IKKa^{SS}\left[1 - \frac{1}{2} e^{-\frac{K_T}{2}\hat{t}}\left((1+\alpha)e^{-\frac{d}{2}\hat{t}} + (1-\alpha)e^{\frac{d}{2}\hat{t}}\right)\right] \tag{S7}$$

$$IKKa^{SS} = \frac{1}{1 + \frac{1}{k_1'} + \frac{1}{k_3'}} \tag{S8}$$

$$K_T = 1 + k_1' + k_3' \tag{S9}$$

$$d = \left((k_1' - (1 + k_3'))^2 - 4k_3'\right)^{\frac{1}{2}} \tag{S10}$$

$$\alpha = \frac{1 - k_3' + k_1'\left(\frac{2}{k_3'} + 1\right)}{d} \tag{S11}$$

The solution can be written in terms of trigonometric or hyperbolic functions depending on whether *d* is real or imaginary but we consider the form above makes the asymptotic behavior easier to appreciate.

General observations

The solution consists of a steady state and a transient part (second term in the square brackets) that decays as $e^{-K_T/2}$. Overshoots occur when the quantity in the second term becomes negative, thus this quantity can be used to define monotonic and adaptive regimes. The parameter plane can be divided in regions according to the asymptotic behavior of α and *d* (Fig. S2), which in terms determine the type of IKKa dynamics. The white region (Fig. S2) corresponds to an imaginary *d*.

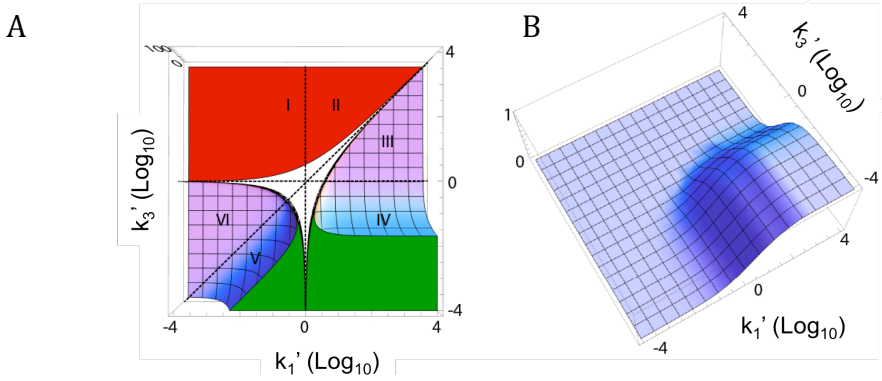

Figure S2. Quantity *d* and transient magnitude. (A) Quantity *d* as a function of k_1' and k_3'. In the red region $d<0$. (B) Magnitude of the overshoot (second term in the square brackets in Eq. S7) scaled by IKK^{SS}. The surface shows significant overshoot for $k_3'<1$ and $k_1'>1$.

In regions I and II, α tends quickly to -1; the first term in the transient drops and the solution becomes strictly monotonic. In both regions *d* is well approximated by $k_3'-1$ and thus the solution takes the form:

$$IKKa[\hat{t}] \sim IKKa^{SS}\left(1 - e^{-\hat{\delta}\cdot\hat{t}}\right)$$
$$\hat{\delta} = 1 + \frac{k_1'}{2} \tag{S12}$$

In region III, when $k_1'>>1$ and $k_3'>>1$, alpha~1 and the cycle response is virtually monotonic ($\delta = k_1+2k_2$ in this limit). In IV, $\alpha \sim k_3'^{-1}$ and the response becomes adaptive with significant overshoots (Figure S2 B). In regions V and VI, d quickly tends to 1 away from the d=0 line. The quantity α tends to $1+2k_1'/k_3'$, which becomes $\sim 2k_1'/k_3'$ in V and ~1 in VI leading again to a monotonic response when $k_1'<<1$. These limits and figure S1 B can be used to define the regions corresponding to each regime: weak activation ($k_1'<10^{-1}$), monotonic ($k_3'>10^{1}$), semi-adaptive ($10^{-1}<k_3'<10^{1}$), and adaptive ($k_3'<10^{-1}$). These definitions are somewhat arbitrary (the monotonic region include responses that are strictly quasi-monotonic) but constitute a useful framework to characterize the motif.

Peak amplitude and weak activation limit

For $k_1' <<1$, the steady state levels of active IKK can be approximated by:

$$IKKa^{SS} \approx \frac{1}{\frac{1}{k_1'}+\frac{1}{k_3'}} \xrightarrow{k_1'<k_3'} k_1' << 1 \qquad \text{(S13)}$$

We found that the maximum of the solution of the differential equations with $k_3'=0$ (effectively neglecting the impact of the recycling reaction during the initial buildup) was a reasonably good estimate for the peak amplitude in adaptive and semi-adaptive regimes. Peak amplitude is almost an exclusive function of k_1' (Fig. S3), especially for $k_1' >\sim k_3'$ or $k_3'<1$.

$$IKKd^{Peak} \approx k_1^{-\frac{1}{k_1-1}} \qquad \text{(S14)}$$

For $k_1'<<1$, the amplitude of the peak ~ k_1'. In this low activation limit, both peak and steady state levels are very low and the biological relevance of the regime is determined by the sensitivity of the downstream target.

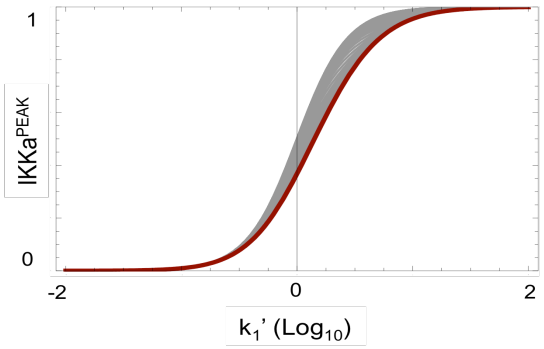

Figure S3. Peak dose response as function of k_1'. The approximate value for Eq. S14 (red line) is compared to the dose responses determined from the simulations for the values of k_3' in Fig. 2 (gray lines). Equation S14 approximates well the peak dose response for low values of k_3' (adaptive and semi-adaptive regimes) but deviations occur for higher k_3' values.

Steady state and peak dose responses

An alternative expression for the steady state concentration of IKKa (Eq. S8) is:

$$IKKa^{ss} = \beta \frac{k_1'}{\beta + k_1'}; \beta = \frac{k_3'}{1 + k_3'} \quad \text{(S15)}$$

From this expression, it is clear that for a fixed k_3', the maximum steady state level of active IKK is achieved as k_1' tends to infinity and is given by β. Then, for each value of k_3', a $k_1'^{ss50}$ value can be defined as the value of k_1' that results in an $IKKa^{SS}$ level equal to half the maximum $IKKa^{SS}(k_1' \to \infty)$. It is straightforward to show that:

$$k_1'^{SS50} = \beta = \frac{k_3'}{1 + k_3'} \quad \text{(S16)}$$

Similarly, a $k_1'^{Peak50}$ can be defined as the value of k_1' that for a given value of k_3' produces a peak of half maximal amplitude. It is relatively straightforward to show from the analytical solution (Eq. S7) that maximum peak amplitude (or steady state levels in strictly monotonic regimes) tends to 1 as k_1' tends to infinity regardless of the value of k_3'. Because of this, $k_1'^{Peak50}$ can be calculated as the value of k_1' that, for a given k_3', produces a maximum IKK activation of 0.5. We do not have a general closed form solution for the exact peak amplitude in terms of k_1' and k_3' that we could invert but from Fig. S4 it is clear that even though the peak amplitude depends strongly on k_1 ($k_1'^{Peak50}$ is ~1) the dependency on k_3' is much weaker. Because of this we calculated $k_1'^{Peak50}$ numerically as the value of k_1' that produce maximum activation of 0.5 for a given k_3' (Fig. S4).

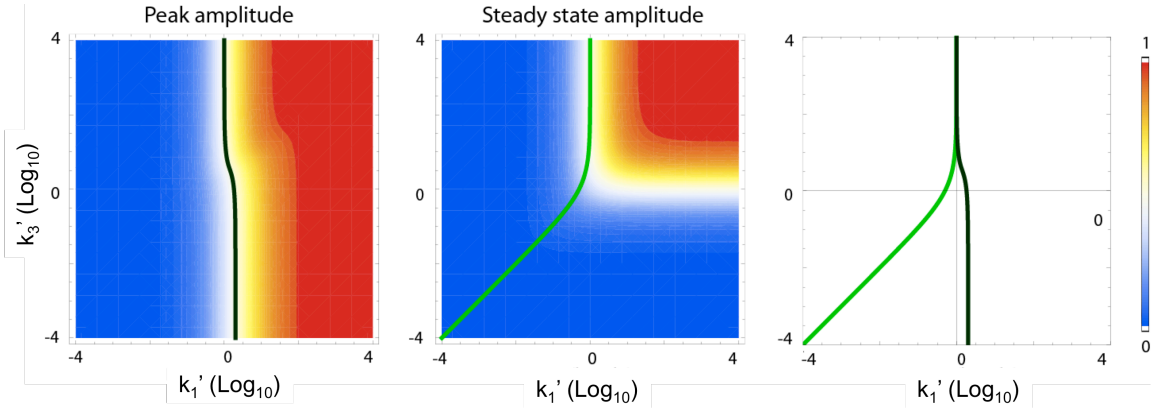

Figure S4. Peak (left) and steady state (center) concentrations of IKKa as a function of k_1' and k_3'. The $k_1'^{ss50}$, and $k_1'^{Peak50}$ curves (light and dark green respectively) are indicated (right).

Peak timing

The time to reach peak activity t^{PEAK} and the level of peak IKK activity, IKK^{PEAK}, can be estimated for adaptive regimes by finding the maximum of the solution of the differential equations with $k_3'=0$. This approximation yields (in k_2 units):

$$t^{PEAK} = \frac{\ln(k_1')}{k_1' - 1} \tag{S17}$$

$$IKK^{PEAK} = k_1'^{-\frac{1}{k_1' - 1}} \tag{S18}$$

This approximation is accurate for adaptive regimes but significant deviation occurs for $k_3'>10$. A similar estimation can be made for monotonic regimes by solving the differential equations neglecting IKKi accumulation ($k_3'\to\infty$). The result is a monotonic increase in IKKa accumulation given by:

$$IKKa = \frac{k_1'}{1 + k_1'}\left(1 - e^{-(1+k_1')\hat{t}}\right) \tag{S19}$$

Here, maximum IKKa corresponds to steady state and is approached asymptotically as time $t\to\infty$. However, the time it takes IKK to reach (100-ε) % of steady state value t^{ε} can be used to estimate a more biological relevant time-scale that can be compared with t^{PEAK}. In units of k_2, t^{ε} is given by:

$$t^{\varepsilon} = -\frac{\ln(\varepsilon)}{1 + k_1'} \tag{S20}$$

Duration dose response

The activation lag can be estimated from the solution of the differential equations with k_3' set to zero.

$$\delta ti = \frac{\ln\left(1 - \frac{\xi^{-1} \times (1 + k_1')}{k_1'}\right)}{1 + k_1'} \tag{S21}$$

This approximation is accurate for small thresholds or adaptive regimes (Fig. 3B in main text) but deviates from the exact value at higher k_3' values.

The delay caused by the time it takes IKK to decay below the threshold once stimulation is terminated was calculated by setting $k_1'\to 0$ in equations 1-3 and solving the resulting exponential decay for the time the concentration of IKKa fell from the IKK^{tp} (level of IKK at the end of the pulse) to the threshold ($1/\xi$) (Eq. S22).

$$\delta td = \ln(\xi) + \ln\left(IKKa^{tp}\right) \quad \text{(S22)}$$

During the rising phase of the response $IKKa^{tp}$ increases with tp. This causes inputs terminating during this period (assuming they are sufficient to drive IKKa over the threshold) to produce outputs with termination delays that grow with tp (Fig. 3 C, main text) leading to the "temporal amplification" phenomenon. During the decaying phase of adaptive responses $IKKa^{tp}$ decreases with tp and thus inputs terminating during this period will see decreasing termination delays as input duration increases. This effect leads to the "blind spot" plateaus in the duration dose response curves.

When the input pulse is long enough to drive the cycle to steady state, IKK^{tp} can be replaced by the expression for IKK^{SS} (the steady state concentration, Eq. S8) yielding:

$$\delta td = \ln(\xi) - \ln\left(1 + \frac{1}{k_1'} + \frac{1}{k_3'}\right) \xrightarrow[k_3'<<1]{} \ln(\xi) - \ln\left(\frac{1}{k_3'}\right) \quad \text{(S23)}$$

In adaptive systems, $k_3'<1$ and if $k_1' \geq 1$, then k_1' can be neglected and the lag becomes independent of the stimulus amplitude.

Response to repeated stimulation

The frequency at which the cycle stops producing full responses to repeated stimulation can be estimated calculating the time it takes to regenerate an almost full amount of poised IKK. In adaptive and semi-adaptive regimes, the rate limiting barrier is recycling from the refractory state and therefore a good estimate of the minimum inter-pulse period that would allow for a fraction of 1-γ in the poised state is:

$$t_{recovery} = \frac{-1}{k_3'} \ln\left(\gamma \times \left(1 + k_3'/k_1' + k_3'\right)\right) \quad \text{(S24)}$$

This expression is for transformed time and the derivation is based on the time it takes the fractional steady state level of IKKi ($IKKi^{SS}=IKKa^{SS}/k_3'$) to decay to γ. The smaller k_3', the longer lived IKKi is, and the longer the recovery time. For pulses shorter than the adaptation time-scale, the time it takes $IKKa^{tp}$ to decay to IKKi must be factored in. For monotonic and quasi-monotonic regimes, the relevant time scale is that of decay from IKKa->IKKi (determined by k_2) and thus $IKKa^{SS}$ must be used as the initial concentration resulting is a slightly modified expression (the k_3'/k_1' term is replaced by $1/k_1'$ and the k_3' in the denominator must be replaced by 1).

In strongly adaptive regimes, when in steady state, the lack of IKK available in the poised state acts as a natural filter for noise present in the input signal. For semi-adaptive regimes in steady state, $IKKi^{SS} > IKK^{SS}$ (this holds when $k_3'<k_1'$ as $IKKi^{SS}=IKKa^{SS}/k_3'$ and $IKK^{SS} = IKKa^{SS}/k_1'$. This is typically the case in semi-adaptive

regimes outside of the weak activation limit) thus limiting the effect of noise in those cases. The effect of noise in the amplitude of the steady state can be gauged by the amount of IKK^{SS} available ($IKK^{SS} = IKKa^{SS}/k_1'$), which can be very small in semi-adaptive regimes subject to strong inputs.

Integral of the signals as information carriers

In adaptive regimes, the integral of the output is a good carrier of amplitude information. This is because the amplitude of the cycle's output depends of the level of upstream activity but its duration is constrained by the adaptive process. In fact, for long enough signals (sufficient to drive the cycle to steady state), the integral of the output is a sigmoid curve that depends only on k_1' (Fig. S5, left panel). In semi-adaptive regimes this is no longer the case as the adapted fraction of IKK contributes to the integral linearly for as long as the input pulse is present (Fig S5, center panel). In monotonic regimes both amplitude and duration contribute to the integral on an equal basis and therefore amplitude can only be unambiguously tracked by the integral of the output if the pathway can be assumed to produce inputs of fixed duration.

Conversely input duration can be tracked through the integral of the output of a cycle operating in the monotonic regime only if amplitude of the input signal can be considered known. This could arise if an upstream regulator operates at saturation at any physiological concentration of the stimulus. In the other regimes, the integral of the output is a poor carrier of duration information because in semi- and adaptive regimes the bulk of the integral is generated by the early phase of the output, which may severely desensitize this metric to subsequent signaling (Fig. S6).

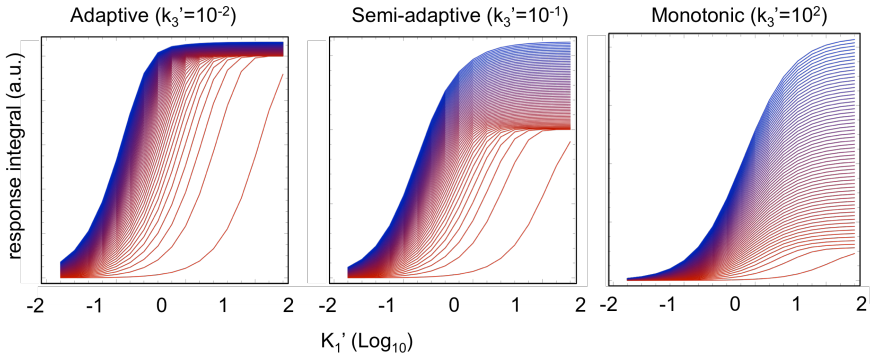

Figure S5. (A) Integral of the three-cycle output for three operating regimes versus input (square pulse) amplitude (k_3' =10^2, 10^0, 10^{-2}, left to right) and increasing duration (red=0.05 to blue=8 in transformed time).

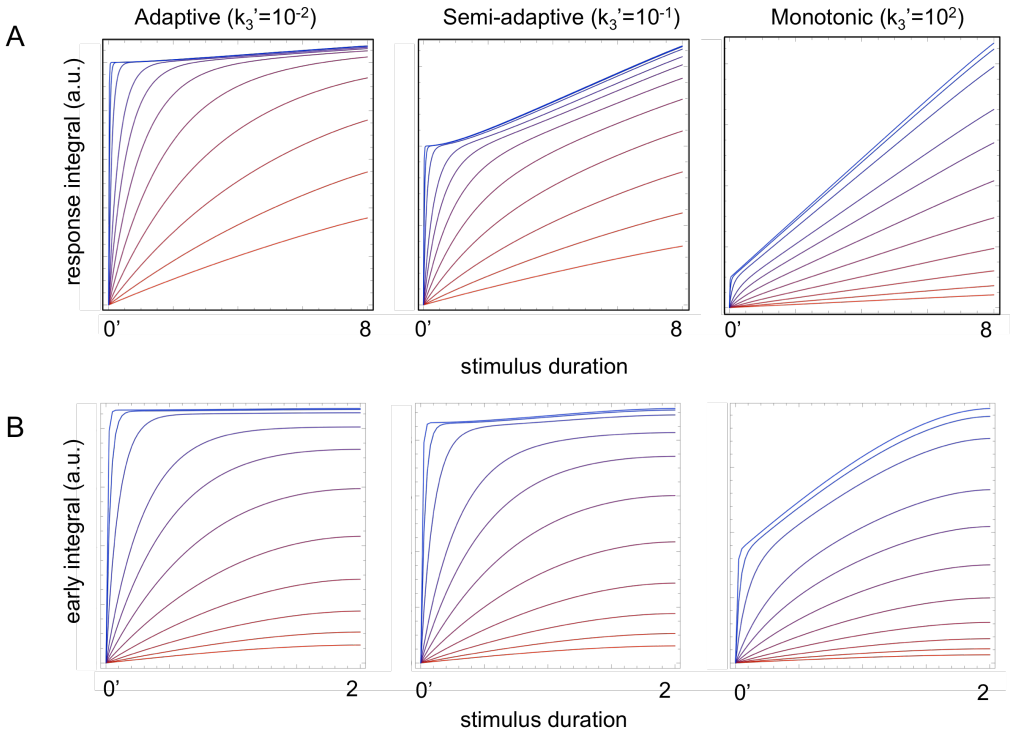

Figure S6. Integral of the output as carrier of input duration information. (A) Integral of the IKK output as a function of duration for square step inputs of different amplitudes (k_1'=10^{-2}-10^{2} red/blue) and three regimes (k_3' =10^{2}, 10^{0}, 10^{-2}, left to right). (B) Same as A but limited to the early phase.

Transfer of duration information by the NFκB pathway

We also analyzed the cycle's ability for transferring information about stimulus duration by measuring the period of time for which IKK and NFκB active fractions remain over 5% of the total available protein. The input duration was defined as the period of time the stimulus level remains over 0.1 (arbitrary units), level that roughly generates a 5% active fraction of IKK (see dose response curves in Fig. 2). Consistent with previous results, for short input pulses, the duration of the IKK signal can deviate significantly from the duration of the input (Fig. S7) whereas for longer lasting ones, IKK is able to accurately track input activity. Interestingly, we observed that for IKK signals lasting between 75 and 150 minutes, the resulting NFκB signal is consistently shorter lived than that of IKK. For longer-lasting signals, the duration of the NFκB response is proportional to the duration of the IKK signal although there is a significant deviation (~45 minutes). These effects seem to compensate for each other as the experiment shows that the duration of the NFκB response varies linearly with the duration of the input (although with a significant delay) for inputs as short as 100 minutes whereas linear relationship between the duration IKK activity and input duration is observed for input signals lasting more than 150 minutes (Fig. S7 right-most panel).

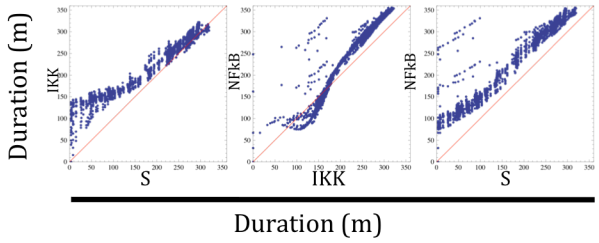

Figure S7 Input vs. output duration (time over 5% activity, see text) for the individual signaling stages (input->IKK, IKK->NFκB) and the combined pathway (input->NFκB).

The multi-state IKK cycle can be reduced to a three state cycle

The kinase IKK is a complex of two catalytic subunits, IKK-alpha and beta, and the regulatory subunit IKK-gamma (also known as NEMO). Current models of IKK regulation include several stages of complex formation and dissociation, as well as phosphorylation and ubiquitination of components (2). In the more detailed model (Fig. S8 A), stimulation induces the recruitment of the IKK-NEMO complex to upstream effectors in a manner thought to be regulated by members of the TRAF protein family. This process promotes the oligomerization of multiple IKK-NEMO units (pre-activation) and the subsequent phosphorylation of IKK activation loop by upstream kinases in a signal-dependent manner. IKK is also thought to be capable of undergoing autophosphorylation independently of upstream kinase activity. In this state, the IKK-NEMO complex is fully active and capable of phosphorylating members of the IκB protein family, causing their rapid degradation and freeing NFκB to translocate to the nucleus. At the same time, the active IKK complex undergoes further trans-autophosphorylation, a process that leads to its breakup (6) and terminates its ability to phosphorylate IκB. In order to be re-activated, the hyper-phosphorylated components need to be dephosphorylated and reassembled into a poised complex in a process that is thought to depend on phosphatases such as PP2A (4) and foldases such as HSP90 (7,8).

The expanded model can be described by the following equations:

$$\frac{d[IKKpa]}{dt} = k_1 \times s_1 \times [IKKc] - k_{2a} \times [IKKpa] \times s_2 - k_{2b} \times [IKKpa] \times [IKKa] \quad \text{(S25)}$$

$$\frac{d[IKKa]}{dt} = k_{2a} \times [IKKpa] \times s_2 + k_{2b} \times [IKKpa] \times [IKKa] - k_3 \times [IKKa] \quad \text{(S26)}$$

$$\frac{d[IKKhp]}{dt} = k_3 \times [IKKa] - k_4 \times [IKKhp] \quad \text{(S27)}$$

$$\frac{d[IKKdp]}{dt} = k_4 \times [IKKhp] - k_5 \times [IKKdp] \quad \text{(S28)}$$

$$\frac{d[IKKc]}{dt} = k_5 \times [IKKdp] - k_1 \times s_1 \times [IKKc] \quad \text{(S29)}$$

, where the sub-indices in the IKK names represent: pa: pre-activated, a: active, hp: hyper-phosphorylated, dp: dephosphorylated, c: competent for activation. S_1 and S_2 represent the two input branches.

The analysis of an expanded model in terms of its amplitude and duration dose responses to synchronized input signals produced results that were virtually indistinguishable from the three-state case for moderate and high stimulus doses (Fig. S8 B-E). Therefore, the expanded model is equally capable of transferring information about the stimulus, with the same limitations that the three-state cycle.

We then focused on the effect of the positive feedback. We observed that even with synchronized signals driving both pre- and activation, the system can respond with a lag that preceded activation in response to low dose inputs (Fig. S8 F). The presence of this lag depends on the relative strength of auto- and stimulus-dependent phosphorylation as an initial amount of active IKK must build up before the feedback begins contributing to activation. Consequently, the activation lag was more evident when stimulus-driven phosphorylation was weak and therefore the feedback branch dominated the phosphorylation process (Fig. S8 F). The duration of the lag depends on the activity of the parallel stimulus-driven branch, with weaker activity producing longer delays. Further weakening of the stimulus-responsive branch led to a diminished overall response. We observed that increasing the rate of pre-activation was not sufficient to compensate for weak stimulus-driven activation and fully eliminate the delay although it contributed to increase the amplitude of the response. The existence of an activation lag clearly precludes the early phase of the expanded cycle response from transferring information about the duration of transient stimulus but leaves the properties of the late phase in terms of information transfer largely unaffected.

Taken together, these observations indicate that the sensitivity and dynamics of the expanded cycle are controlled by a balance between pre-activation, self-, and stimulus-induced phosphorylation in an intricate manner. Depending on the details of how the stimulus decay as well as on the kinetic laws applicable to the reactions in the cycle, multiple phases with transient over- or under-shots are possible especially when the inputs are non-synchronous. As the dynamics of IKK's upstream effectors are not yet well established, we will not study these more complex scenarios further.

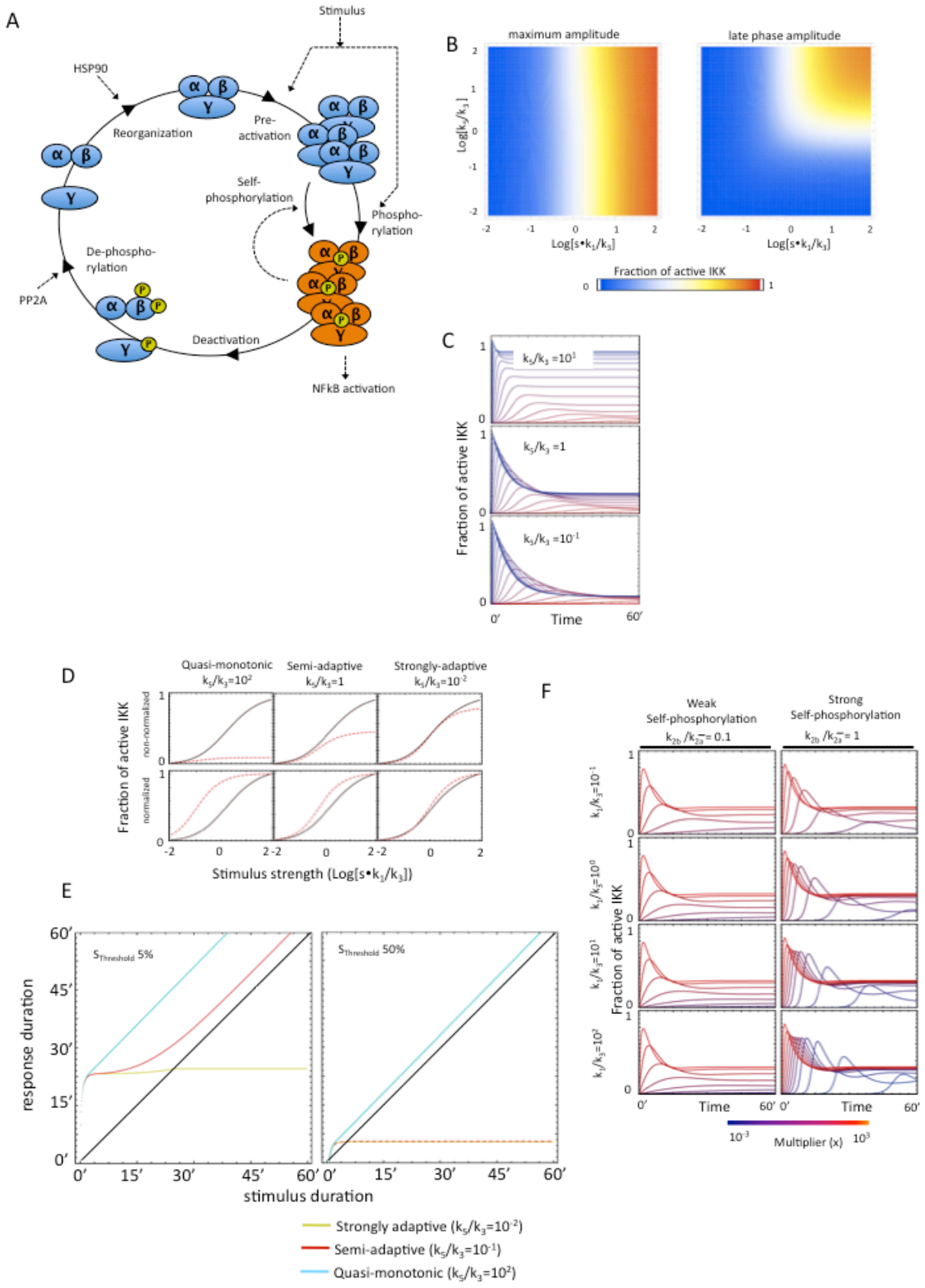
A
Stimulus
HSP90
Reorganization
Pre-
activation
Self-
phosphorylation
Phospho-
rylation
De-phospho-
rylation
PP2A
Deactivation
NFkB activation
B
maximum amplitude
late phase amplitude
Log[k5/k3]
Log[s•k1/k3]
Fraction of active IKK
C
k5/k3 =10^1
k5/k3 =1
k5/k3 =10^-1
Fraction of active IKK
Time
0′
60′
D
Quasi-monotonic
k5/k3=10^2
Semi-adaptive
k5/k3=1
Strongly-adaptive
k5/k3=10^-2
non-normalized
normalized
Fraction of active IKK
Stimulus strength (Log[s•k1/k3])
E
S Threshold 5%
S Threshold 50%
response duration
stimulus duration
Strongly adaptive (k5/k3=10^-2)
Semi-adaptive (k5/k3=10^-1)
Quasi-monotonic (k5/k3=10^2)
F
Weak
Self-phosphorylation
k2b /k2a = 0.1
Strong
Self-phosphorylation
k2b /k2a = 1
k1/k3=10^-1
k1/k3=10^0
k1/k3=10^1
k1/k3=10^2
Fraction of active IKK
Time
Multiplier (x)
10^-3
10^3

Figure S8. An extended IKK model. (A) In a more detailed model of IKK regulation, resting cells contain IKK-NEMO in an inactive conformation. Following signal onset, the complex undergoes a conformational change and oligomerization that result in a pre-activated complex. The complex becomes accessible for IKK kinases (e.g. TAK1) in addition to undergoing autophosphorylation. In this state, the IKK-NEMO complex is fully activated and phosphorylates the IκB proteins as well as residues within the complex. The latter trans-autophosphorylation step leads to the breakup of the NEMO-IKK complex. These hyper-phosphorylated forms are dephosphorylated by phosphatases (e.g. PP2A) and the IKK-NEMO complex reassembles aided by foldase HSP90. (B) The model was stimulated with square-step stimuli of varying amplitude and maximum and late phase amplitude were determined as a function of the normalized stimulus strength ($k_1 s/ k_3$) and recycling rate (k_5/ k_3) parameters.(C) Typical temporal profiles of IKK activity at various stimulus amplitude for the three regimes ($k_5/ k_3 = 10^2, 10^0, 10^{-2}$) for a cycle in which the stimulus-dependent branch dominates phosphorylation. (D) Amplitude dose response curves for the five-state IKK model for the three regimes. The lower panels show the dose responses normalized to their maximum attained value. (E) Duration of the cycle response (defined as in Fig. 3) to square pulses of saturating amplitude for the three regimes.(F) Typical time courses of fully active IKK in response to square step stimuli for two cycles with weaker (left) and stronger (right) self-phosphorylation branches (k_{2b} is the rate constant for the self-phosphorylation reaction and k_{2a} is the unperturbed rate of the stimulus-dependent phosphorylation branch). The color scale indicates the value of a multiplier "x" applied simultaneously to both stimulus-dependent reactions in the model. The rows correspond to different values of the unperturbed pre-activation parameter k_1 and illustrate that even though the sensitivity of the cycle can be improved, the activation delay is not fully eliminated.

References

1. Kishore, N., C. Sommers, S. Mathialagan, J. Guzova, M. Yao, S. Hauser, K. Huynh, S. Bonar, C. Mielke, L. Albee, R. Weier, M. Graneto, C. Hanau, T. Perry, and C. S. Tripp. 2003. A selective IKK-2 inhibitor blocks NF-kappa B-dependent gene expression in interleukin-1 beta-stimulated synovial fibroblasts. J Biol Chem 278:32861-32871.

2. Hayden, M. S. and S. Ghosh. 2008. Shared principles in NF-kappaB signaling. Cell 132:344-362.

3. Delhase, M., M. Hayakawa, Y. Chen, and M. Karin. 1999. Positive and negative regulation of IkappaB kinase activity through IKKbeta subunit phosphorylation. Science 284:309-313.

4. Kray, A. E., R. S. Carter, K. N. Pennington, R. J. Gomez, L. E. Sanders, J. M. Llanes, W. N. Khan, D. W. Ballard, and B. E. Wadzinski. 2005. Positive regulation of IkappaB kinase signaling by protein serine/threonine phosphatase 2A. J Biol Chem 280:35974-35982.

5. Werner, S. L., D. Barken, and A. Hoffmann. 2005. Stimulus specificity of gene expression programs determined by temporal control of IKK activity. Science 309:1857-1861.

6. Palkowitsch, L., J. Leidner, S. Ghosh, and R. B. Marienfeld. 2008. Phosphorylation of serine 68 in the IkappaB kinase (IKK)-binding domain of NEMO interferes with the structure of the IKK complex and tumor necrosis factor-alpha-induced NF-kappaB activity. J Biol Chem 283:76-86.

7. Broemer, M., D. Krappmann, and C. Scheidereit. 2004. Requirement of Hsp90 activity for IkappaB kinase (IKK) biosynthesis and for constitutive and inducible IKK and NF-kappaB activation. Oncogene 23:5378-5386.

8. Hinz, M., M. Broemer, S. C. Arslan, A. Otto, E. C. Mueller, R. Dettmer, and C. Scheidereit. 2007. Signal responsiveness of IkappaB kinases is determined by Cdc37-assisted transient interaction with Hsp90. J Biol Chem 282:32311-32319.